Precast Segmental Bridge Columns with Resettable Sliding Joints —— An Inspiration from Ancient Chinese Pagodas

Y.Q. Liu[1*], F. Liang[1], Francis T.K. Au[1]

[1]Department of Civil Engineering, The University of Hong Kong, Hong Kong, China

The construction of bridge substructures by in-situ assembly of precast concrete segments provides significant benefits in quality control and economy, but their seismic stability is always a concern. Incidentally, prefabricated components have long been used in building tall pagodas for thousands of years in China. Among the pagodas that have survived numerous centuries, the timber pagodas are believed to be assembled structures of great research value in respect of seismic isolation design. There is indeed a certain degree of similarity between the timber pagodas and the proposed precast segmental bridge columns with resettable sliding joints. The smart seismic isolation mechanism in multi-storey timber pagodas with mortise-tenon rocking columns and distributed bracket sets has the following key features: (a) high lateral flexibility, (b) smart energy dissipation system, (c) guided self-centring behaviour, and (d) measures to enhance vertical stability. Actually, the resettable sliding joints in the present precast segmental bridge columns are so designed and distributed to obtain a similar seismic isolation mechanism. Time-history simulation results of seven conceptual models show that the columns with resettable sliding joints outperform the other counterparts especially in respect of (a) the overall seismic isolation between the top mass simulating the deck and the shaking ground, (b) the control of residual sliding displacements at segment interfaces, and (c) satisfactory energy dissipation performance.

Keywords

Earthquakes, mortise-tenon joints, resettable sliding joints, segmental structures, seismic isolation

1. Introduction

Precast concrete segmental construction is one of the popular methods of accelerated bridge construction, which can cover not only the decks of bridges of short-to-medium spans, but also the columns. The success in segmental bridge column construction in the low-seismicity regions has prompted research work of seismic-resistant segmental columns [1] having non-emulative joints that are basically dry connections between segments allowing possible separation. The gap opening between segments, carefully controlled by mono-strand [2,3] or multi-strand [4] tendon systems, has been utilized to incorporate rocking behaviour into the segmental columns so that a higher drift ratio can be reached. Apart from gap opening, subsidiary sliding behaviour has also been wisely combined into the rocking segments with hybrid sliding-rocking joints [5]. The potential of improved seismic performance is well recognised by the use of assembled columns [6-10] or frames [11-15] with precast segments.

Actually, seismic design and construction has been a long-standing field of structural engineering, as evidenced by the devastating damage caused by countless earthquakes over the centuries. Among numerous ancient assembled structures that have survived natural disasters over their long history, the Yingxian timber pagoda is believed to be of great research value due to its extensive adoption of a special type of bracket sets (known as *Dou-gong*) and mortise-tenon joints [16]. Despite the use of different arrangements of these components, results of shaking table tests of the scale models of a pagoda [17] and a tower [18] incorporating these bracket sets and mortise-tenon joints showed similar trends of dynamic properties. The structural frequencies identified decreased noticeably during the severe part of ground shaking but they largely recovered afterwards. To explain this phenomenon, quasi-static tests were also carried out on typical bracket sets [19,20], timber frames with mortise-tenon joints [21-23], and the whole system [24].

Despite their inspiring discoveries, most of the above experiments were primarily intended to improve the preservation and maintenance of historical timber structures. In an attempt to extend the application of precast segmental bridge columns to regions of moderate to high seismicity, resettable sliding joints are introduced. Striking similarity is observed in the dynamic behaviour of pagodas and precast segmental bridge columns with resettable sliding joints. In this paper, the smart seismic isolation mechanism in multi-storey timber pagodas with mortise-tenon rocking columns and distributed bracket sets is elaborated with emphasis on the theory behind. Incidentally,

the resettable sliding joints are so designed and distributed in the current version of precast segmental bridge columns so as to achieve a similar seismic isolation mechanism between the bridge deck and the ground.

2. Seismic isolation mechanism in ancient Chinese pagodas

Since Buddhism was introduced to and embraced in China thousands of years ago, many pagodas were built in the form of assembled structures. These pagodas had increased a lot in size with improvements in design concept and construction technology during the Song Dynasty (960-1279AD), as the heights of pagodas were in some way regarded as the symbol of national strength in comparison with its powerful neighbouring empire of Liao (916-1125AD) in the north. As the highest ancient timber structure in China, the Yingxian pagoda in Shanxi Province of Northern China as shown in Fig. 1 has gone through earthquakes of magnitudes ranging from 4 to 7 on the Richter scale for over 50 times in the past 1000 or more years [16]. However, it still remains in good conditions as a historic site for tourists till now, making it a masterpiece on the extensive use of bracket sets and mortise-tenon joints.

Fig. 1. The Yingxian timber pagoda, Shanxi Province, China [25]

As the old saying goes, nine out of ten ancient pagodas are tilted. This is somehow related to the flexibility of pogodas with distributed bracket sets and mortise-tenon rocking columns. This lateral flexibility also contributes a certain degree of seismic isolation to the whole structure during earthquakes. This recoverable seismic isolation mechanism can be briefly summarized as providing (a) adaptive lateral flexibility; (b) smart energy system; (c) guided self-centring behaviour; and (d) countermeasures for vertical instability.

2.1. Adaptive lateral flexibility

Unlike modern structures where deformations are largely associated with material properties, connections in ancient Chinese timber structures had allowed some degrees of freedom, resulting in semi-rigid joints. Therefore deformations can be easily attained without causing much damage in the material itself. Like the typical mortise-tenon connections as shown in Fig. 2, the typical column is usually freestanding on or lodged inside the recess of a stone base, while the typical beam is having the tenons at the ends inserted into the mortise holes of the adjacent columns to allow slight rotations when they are subjected to external bending moment [26,27].

An interesting finding on this kind of joints is that a larger gap between the mortise and through-tenon will noticeably reduce the initial stiffness as well as the ultimate strength, and the gap would certainly result in some sort of free rotation as the column rocks about its original position [21]. The wooden material is anisotropic and hence

the tenon can deform easily by lateral squeezing by the mortise under severe bending conditions. The enlarged gap between the mortise and tenon caused by severe shaking at the peak stage of an earthquake would render the mortise-tenon joints more flexible compared to the initial state, subsequently resulting in higher lateral flexibility of the whole structure with further earthquake excitation. However, when the earthquake is over, it largely regains its original stiffness.

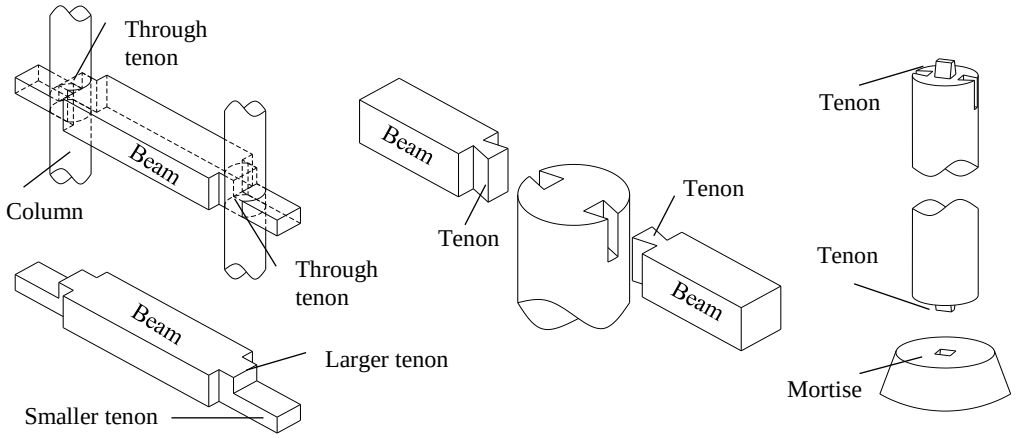

Fig. 2. Typical mortise-tenon connections

2.2. Smart energy system

Investigations on the mortise-tenon joints [28,29,22] and the bracket sets [30] indicated that these joints had good energy dissipation capability, all together contributing to the superior seismic performance of the whole system. An equivalent viscous damping coefficient of above 0.25 could be attained and maintained as drift proceeds to higher values in the mortise-tenon joints, which was attributed to the plastic deformation of the wooden member there [16,17]. Despite a lower equivalent viscous damping coefficient found in the bracket sets, the friction was found to play an important role in the energy dissipation capability of these brackets [19,31].

The high equivalent damping coefficient observed in the ancient Chinese timber structures can also be attributed to the smart store-and-release regime in accommodating vertical movement. It is proved that, despite small vertical displacements, a heavy roof can store a noticeable amount of gravitational energy as it rises along with severe column rocking behaviour and it can release the energy during unloading [24].

Unlike the elastic strain energy of columns in bending, this transferable gravitational energy is mainly released in a vertical manner. It is also inspiring to note that, by means of a thoughtful assembly of segments, the energy from horizontal excitation can be partially transferred vertically through the rocking behaviour. This process is much less likely to cause any dynamic side effects such as resonance.

2.3. Guided self-centring behaviour

The inherent multiple flexibility has indeed enabled ancient timber pagodas to survive strong ground shaking without causing much damage, demonstrating an aspect of their smart seismic isolation mechanism. Moreover, the successful preservation of these pagodas also relies heavily on their satisfactory self-centring capability so that they are in good conditions and equipped with some spare capacity for future natural hazards even without excessive maintenance.

Field survey of many existing pagodas built in the Song Dynasty indicates that the peripheral columns would lean inwards by a small inclination towards the centre [22] as indicated by the arrows in the plan as shown in Fig. 3(a). The peripheral bracket sets always have an interlocking layer arrangement with at least one inclined component with

its higher end pointing towards the centre of the pagoda (Fig. 3(b)). Apparently, this intended arrangement of leaning columns and bracket sets would slightly change the overall rocking behaviour of the pagoda.

This rocking system can be explained theoretically with simplified structural models assuming that all components are rigid bodies and the connections are strong enough to resist the forces involved.

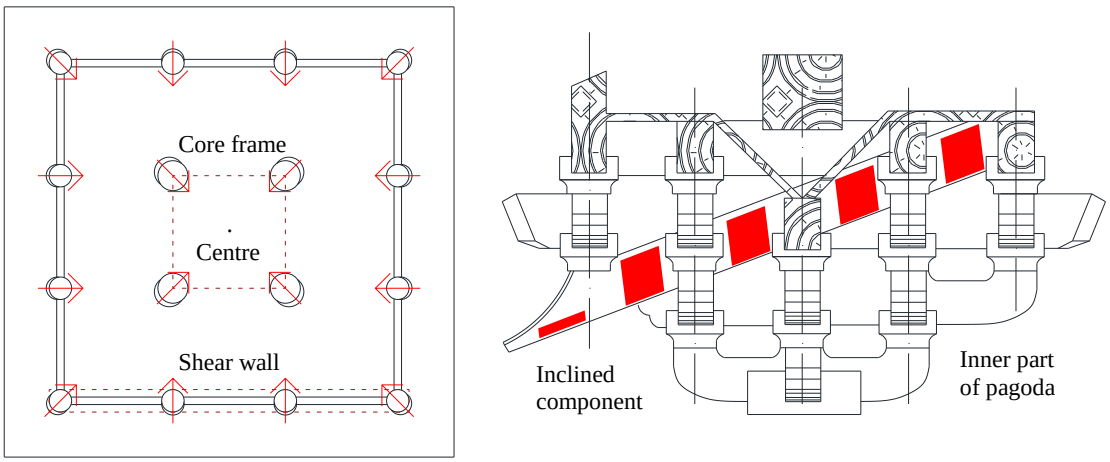

(a) (b)

Fig. 3. Typical arrangement of pagoda (a) floor plan with leaning columns and (b) bracket sets with inclined component

2.3.1. Simplified structural models for leaning columns

Under the rigid body assumption, all the nodes at the mortise-tenon beam-column joints at the column top (e.g. points B and E) share the same horizontal displacement input corresponding to that particular level, as shown in the simplified model for leaning columns in Fig. 4(a). The leaning nature of the columns can make a difference in the vertical uplifting at the top column connections despite the small tilting angle. If the frame in Fig. 4(a) sways to the left, for example, point C will ascend vertically while point F will descend, and vice versa.

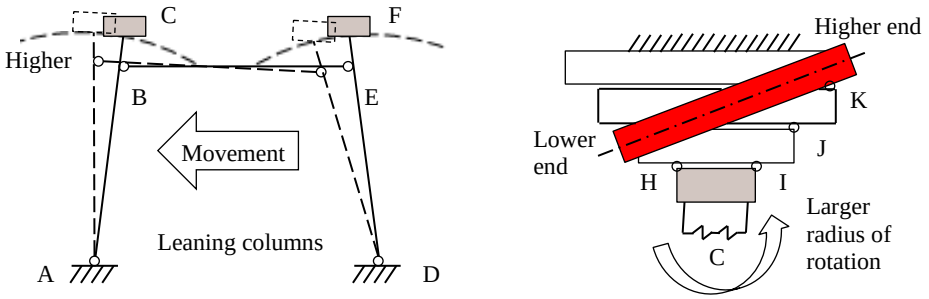

(a) (b)

Fig. 4. Simplified structural models (a) leaning columns and (b) bracket sets with inclined component

2.3.2. Simplified structural models for bracket sets with inclined component

In view of the heavy superstructure, the floors of the pagoda will have very small rotations. Therefore, the rotation of top components of the bracket sets can be effectively considered as being fixed. Owing to the presence of the inclined component inside, the bracket set behaves differently depending on the direction of applied horizontal displacement in the vertical plane containing the inclined component. Every intersection between the perpendicular members as shown in Fig. 3(b) can act like

a hinge to accommodate a certain amount of rotation. The simplified structural model in Fig. 4(b) shows the bracket set comprising several layers stacking together with some potential pivots indicated when the leaning column experiences rotations of different sense.

2.3.3. Overall rocking performance of the combined system

For a simplified overall analysis of the rocking performance of the combined system, the top node of column is rigidly connected to the bottom component of its upper bracket set. In view of the rocking trend in the structural model comprising leaning columns and bracket sets with inclined components as shown in Fig. 5(a), the centroid of the top mass is actually moving along a curved pendulum orbit. More specifically, the uneven uplift of the top mass induced by horizontal rocking of the combined system results in dislocation as well as rotation of the top mass, giving approximately a gently concave quasi-static pendulum orbit of the centroid with the instantaneous centre of the rotation above the top mass. Therefore, it results in stable equilibrium. If the top mass is slightly displaced, it always tends to return to its original position, achieving efficient self-centring performance especially considering the variability of the seismic input.

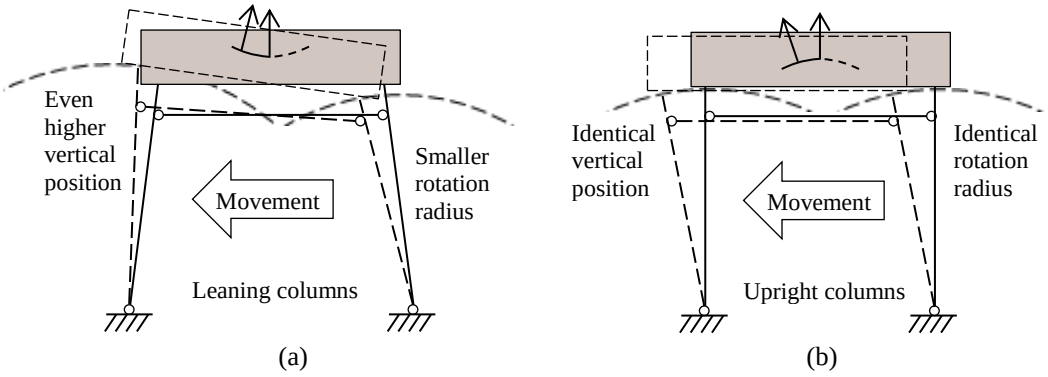

Fig. 5. Top mass motion in combined systems (a) a concave pendulum orbit and (b) a convex orbit

In the structural model comprising upright columns and symmetrical bracket sets without the inclined component as shown in Fig. 5(b), the top mass remains horizontal, giving approximately a gently convex orbit of the centroid with the instantaneous centre of the rotation below the top mass. In comparison, it leads to neutral equilibrium at small displacement or even instability.

2.4. Countermeasures for vertical instability

2.4.1. Vertical instability in the vicinity of bracket set

Potential instability may occur as the top mass is about to move back to its original position from somewhere else along the pendulum orbit dynamically [32]. To tackle such potentially undermining diagonal movements caused by both the horizontal and vertical components of acceleration of the earthquake, the inverted triangular shaped bracket set with intersecting layers of slender timber components can easily accommodate any diagonal displacement by rotation about any interlocking points, e.g. points H, I, J and K in Fig. 4(b), for ground motion in various directions, ensuring that the bracket set can always maintain some contacts between the top mass and the column top during the entire seismic event.

2.4.2. Vertical instability at the column base

Severe excitation from the vertical component of an earthquake may also adversely affect the integrity of the assembled pagodas, but having the columns just sitting on a cornerstone can be a simple yet efficient way to solve it. Permanent dislocation between the column foot and the cornerstone was often observed in relevant experiments and simulations [33], proving that the loss of contact may be concentrated at the column feet during seismic events as if the column foot is bouncing up and down with the shaking.

3. Inspiration for design of precast segmental bridge columns

Traditionally, precast segmental bridge decks and columns used to have epoxy joints to mimic cast in situ construction and ensure the structural rigidity. However, examination of ancient Chinese timber pagodas that have survived numerous earthquakes has provided useful insights into the inherent flexibility of assembled structures. The flexibility of these timber pagodas and their ability to reset after being disturbed have helped them survive numerous centuries. A rethink of the design strategy is hence desirable. Inspired by this smart seismic isolation mechanism, resettable sliding joints have been studied for possible introduction to precast segmental bridge columns considering the common post-peak features of earthquakes [34]. In this design, the segments are able to oscillate about the original position by sliding and possibly rocking for satisfactory seismic isolation during the stage of strong shaking. Moreover, the segments also have the tendency to slide back to the original position under the subsequent excitations of small magnitudes to achieve satisfactory self-centring performance, as if the dislodged segments are reset at the joints upon cessation of an earthquake.

In particular, the resettable sliding joint [35] consists of three major components as shown in Fig. 6: (a) durable low-friction concrete-to-concrete contact surfaces; (b) non-planar contact surfaces with gentle guide keys; and (c) partially debonded tendons with low initial prestress.

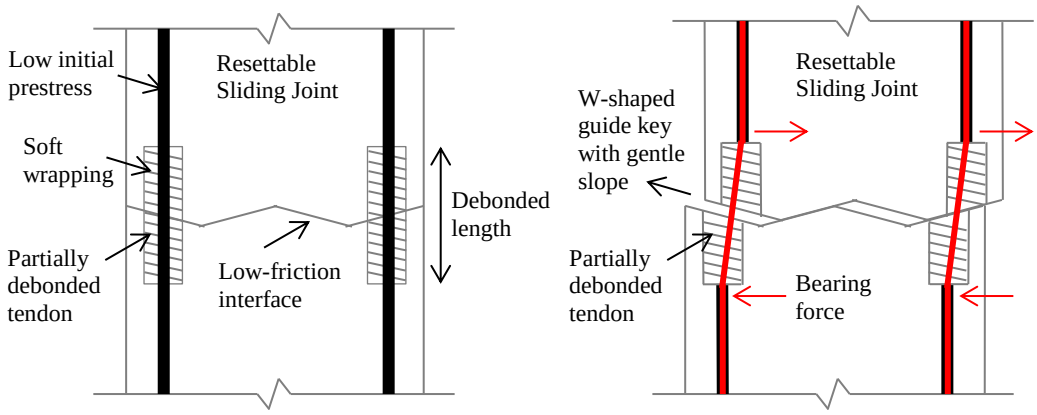

Fig. 6. Major components of the resettable sliding joint

3.1. Low-friction concrete interface

To obtain similar adaptive lateral flexibility as in the timber pagodas with flexible mortise-tenon joints, the concrete contact surfaces of the resettable joint are permitted to slide against each other with a low coefficient of friction (CoF). Incidentally, the friction also helps in dissipating energy during the sliding oscillations due to earthquakes.

Untreated concrete surfaces are porous and prone to dust accumulation and scratches due to scraping because of the remaining lime and aggregates there. Therefore, untreated concrete surfaces are unable to provide low-friction contacts. Nevertheless, a stable CoF below 0.1 has been reported in cyclic shear tests of concrete specimens [36,5], which is low enough to achieve the desirable sliding in the resettable sliding joints. In the research field of tribology, lubrication and wear are two decisive factors to achieve stable low-friction contacts of CoF below 0.05 especially under high contact pressure [37]. With proper treatment of the concrete contact surfaces, it is feasible to achieve a low CoF in the design of resettable hybrid sliding-rocking joints.

3.2. Gentle guide keys

Compared to the pendulum orbit obtained from special rocking behaviour in the pagoda model mentioned earlier in Section 2.3.3, the sliding motion of the segments with resettable sliding joints is more straightforward in view of the shape of the contact surfaces. To provide both the sliding-type self-centring performance and some moment resistance, a section profile with W-shaped gentle guide keys having mild inclination of 2° to 9° may be adopted as shown in Fig. 6.

In comparison, if a V-shaped contact surface is adopted, the upper block will tend to tip about its lower obtuse corner during downslope sliding because of the lack of resisting moment. Although the V-shaped contact surface is more convenient in construction, the seismic behaviour will likely involve both sliding and rocking responses. However, at this initial stage of investigation of resettable sliding joints, the simpler contact surface with W-shaped guide keys is adopted with special emphasis on the sliding-type seismic isolation ability during severe excitations of a seismic event.

3.3. Partially debonded tendons

Fig. 6 shows that the partially debonded tendon comprises a grouted tendon inside a regular duct with a certain length of the duct adjacent to each joint at the contact surface wrapped by an annulus of soft resilient material to allow a certain amount of relative sliding movements at the contact surface during an earthquake. This design not only creates room for relative sliding at the contact surface, but also provides some restoring force to assist in resetting. It is however necessary to provide sufficient operational prestressing force in the tendons considering the inclination of the gentle guide keys in order to avoid any sliding at joints during conditions other than earthquakes.

Moreover, unlike the fully unbonded tendons, the presence of grout not only boosts the durability of tendons but also enhances the interaction between adjacent segments. Flexural cracking or crushing of the grout under excessive sliding oscillation during earthquake is inevitable, but the damage to the grout is considered acceptable during an earthquake.

Table 1 compares the seismic isolation performance of ancient Chinese pagodas and precast segmental columns with resettable sliding joints in respect of the contribution of various components. In particular, the smart store-and-release energy transformation mechanism in the pagodas through the incidental vertical movement of the top mass is largely reproduced in the precast segmental columns with the gentle guide keys in the resettable sliding joints.

Table 1 Comparison between ancient Chinese pagodas and precast segmental columns with resettable sliding joints in respect of seismic isolation

Components	Ancient Chinese pagodas	Columns with resettable sliding joints
Adaptive lateral flexibility	Mortise-tenon beam-column joint	Low-friction concrete interface
Smart energy system	Mortise-tenon beam-column joint (mainly dissipation); bracket sets (transformation)	Low-friction concrete interface (dissipation); gentle guide keys (transformation)
Guided self-centring behaviour	Mortise-tenon beam-column joint; bracket sets	Gentle guide keys; partially debonded tendons
Countermeasures for vertical instability	Bracket sets	Partially debonded tendons

4. Numerical simulations of precast segmental column with resettable sliding joints

To better understand conceptually the dynamic behaviour of precast segmental columns incorporating resettable sliding joints and other typical joints for bridges under seismic loading, simplified numerical simulations are carried out in OpenSees environment [38] with following assumptions:

- The concrete segments are considered as rigid blocks.
- The bridge deck is only considered as an additional mass concentrated at the top of the column.
- Any possible impact between the tendon and the surrounding duct during segment sliding is neglected.
- Outside the debonded length, the tendon will have perfect bonding without failure.

4.1. Model verification

Model verification is carried out using a related problem with available reference solution before applying the method to precast segmental bridge columns with resettable sliding joints. Two major difficulties are encountered in modelling the above resetting sliding joints numerically: (a) capturing the hybrid sliding and rocking interaction between segments with W-shaped inclined contact surfaces, and (b) simulating the behaviour of the partially debonded tendon system for properly considering the participation of adjacent moving segments. It is widely accepted to use the in-built materials with no-tension and tension-gap characteristics in OpenSees [39,40] to simulate possible rocking and tendon behaviour, respectively, in dynamic analyses. Particularly for the guided sliding behaviour, the Flat Slider Bearing Element in OpenSees is utilized in modelling the proposed resetting sliding joints [41], where the global orientation vector to define the sliding surface and user-defined friction model can be easily prescribed.

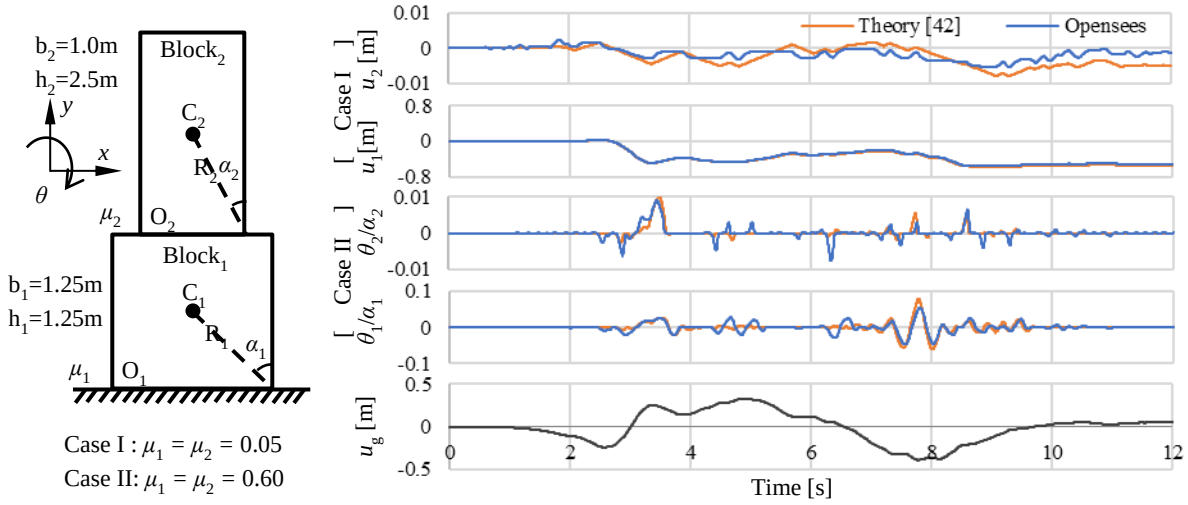

Fig. 7. Theoretical and numerical results of kinematic behaviour of two rigid blocks under excitation

The validation of selected OpenSees elements and methods for capturing the hybrid sliding and rocking kinematic behaviour of stacked rigid blocks is conducted by comparing the simulation results with the reference solution of an existing theoretical model [42]. Fig. 7 shows the theoretical model used, where the lower block has equal breadth and height of $b_1 = h_1 = 1.25$ m, respectively, and the upper block has breadth and height of $b_2 = 1.0$ m and $h_2 = 2.5$ m, respectively. The same value of coefficient of friction at the base applies to both the lower and upper blocks, i.e. $\mu_1 = \mu_2 = \mu$. To examine different response modes, two cases are studied, i.e. $\mu = 0.05$ (smooth) and $\mu = 0.6$ (rough). The ground motion displacement u_g is taken as the first 12 seconds of the S16E displacement component recorded at the Pacoima Dam during the 1971 San Fernando earthquake with a scale factor of 1.0 as shown in Fig. 7. The theoretical model is then analysed by OpenSees using the Flat Slider Bearing Elements with upright orientation vectors.

The rotations of the lower and upper blocks are θ_1 and θ_2, respectively, while the horizontal displacements of the lower and upper blocks are u_1 and u_2, respectively. For convenience in presentation, the rotation is normalised by the angle made between the line joining a corner to the centroid of block to the vertical as shown in Fig. 7, i.e. θ_1/α_1 and θ_2/α_2 for the lower and upper blocks, respectively. The theoretical rotation results for Case II ($\mu = 0.6$) are used for parameter tuning of the OpenSees model, while the theoretical relative sliding results for Case I ($\mu = 0.05$) are used for model validation. Excellent agreement of theoretical and numerical results for the horizontal displacement u_1 of the lower block for Case I is observed in Fig. 7. Note that the discrepancy of the horizontal displacement u_2 of the upper block for Case I is just a few mm, which is extremely small compared with the amplitude of ground motion displacement. The results therefore indicate that the numerical methods used for simulating the sliding joints in OpenSees are reliable, and the tuned parameters of damping and stiffness of the OpenSees Flat Slider Bearing Element for hybrid sliding and rocking contacts can be used for the subsequent dynamic analyses of precast segmental columns with multiple resettable sliding joints.

4.2. Conceptual study of dynamic responses of different precast segmental columns

Fig. 8 shows the OpenSees model of precast segmental column comprising 5 segments for the conceptual study, where the nominal height and breadth of segment are $h = B = 1000$ mm, respectively. As the overall behaviour of the precast segmental column is primarily governed by the deformations of the unbonded parts of tendon, only these unbonded parts are modelled by truss elements and the deformations of the bonded parts of tendon are ignored in this preliminary analysis. In this simplified model, an equivalent top mass is used to simulate the total effective mass of deck and loads carried by the column. The magnitude of the equivalent top mass is reflected by the top mass ratio that is defined as the equivalent top mass to the mass of column, which ranges from a low value of 3 to a higher value of 15 depending on the type of bridge, e.g. highway or railway bridge. The parameter G here denotes the total gravity force acting on the column base. Truss elements with co-rotational geometric transformation and tension-only gap material are used to simulate the tendons, which are installed at the periphery of the section in either fully unbonded or partially debonded condition. For simplicity, the possible failure of anchorage and grout for the tendons is ignored. Flat Slider Bearing Elements with compression-only material and general Coulomb friction model are distributed at the nodes along the W-shaped interfaces defined by orientation vectors. The excitation input of Landers LCN_345 recorded at Station RSN879 is selected and scaled to a maximum peak ground acceleration (PGA) of 1.0g with the corresponding peak ground displacement of 324 mm (about 1/3 of the column width), where g is the acceleration due to gravity. In each case, time history analysis is carried out for at least an additional period of 15 seconds after cessation of earthquake excitation.

The material and contact parameters used in the simulation are determined based on the above validation as given in Table 2. It should be stressed that the simulations presented here are based on largely simplified models with rigid bodies for conceptual understanding of the dynamics of precast segmental columns under seismic input.

Table 2 Material and contact parameters of OpenSees models

Description	Components	Units	Values
Co-rotational Tendon Truss elements	Tension modulus	N/mm^2	7.50E+05
	Initial gap for zero tendon force	mm	-8.27E-04
	Initial gap for 3.0G tendon force	mm	-7.00E-02
Flat Slider Bearing Contact elements	Compression modulus	N/mm^2	7.50E+03
	Coulomb Friction model modulus	N/mm^2	3.50E+02
	Damping coefficient	-	0.02

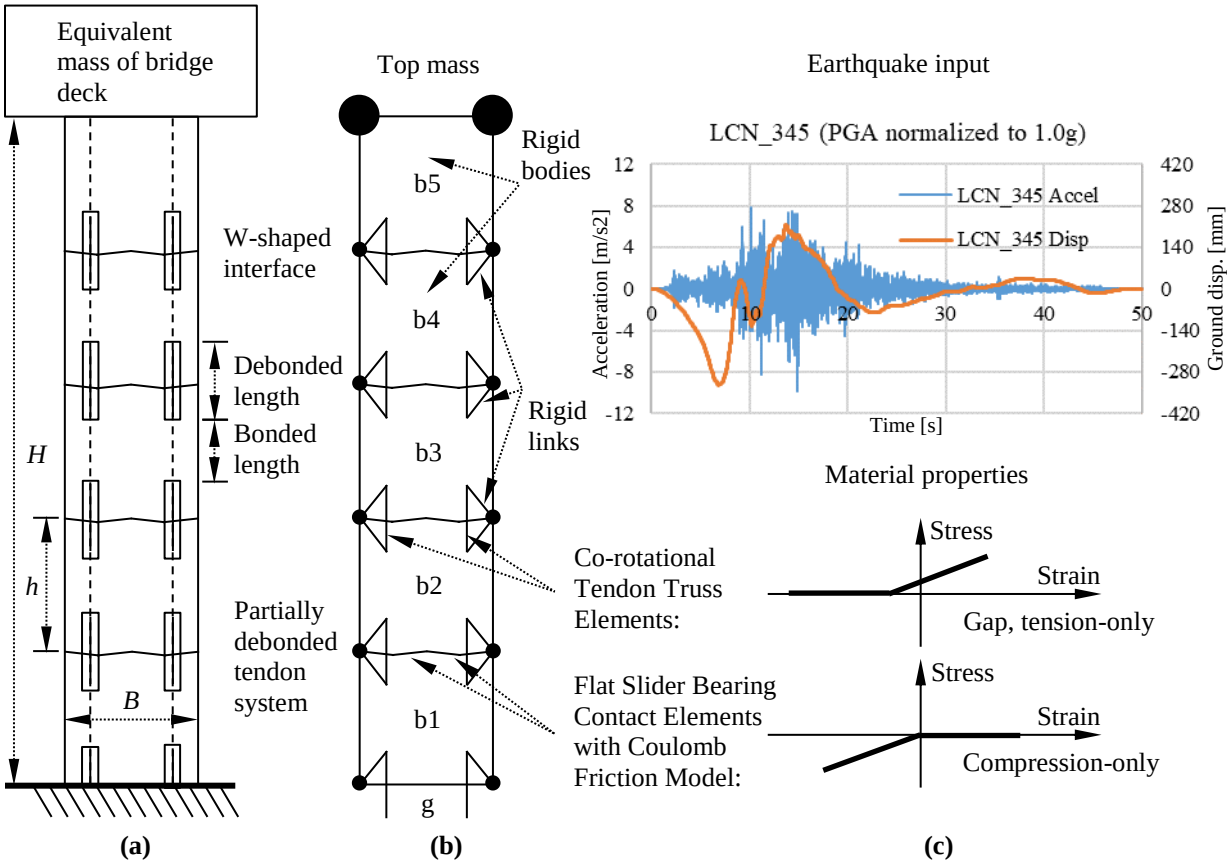

Fig. 8. Precast segmental column with resettable sliding joints: (a) physical system, (b) model in the OpenSees, and (c) information of seismic input and materials

A series of parametric studies are carried out to further investigate the dynamic behaviour of the proposed system. Based on the results of [34], the column in Case No. 1 has adopted resettable sliding joints (RSJ) with low-friction contact (CoF = 0.05) and gentle W-shaped inclination of 3°, which will give reasonably optimal performance. Partially debonded tendons are provided with a negligible initial prestressing force just to keep the tendons taut in most of the cases, while in one case a high prestressing force of 3.0*G* is adopted like the design of [7]. The initial force carried by the tendon truss element can be tuned by adjusting its initial gap value, and the tensile force is monitored subsequently for its variations. In general, only one parameter is modified in each case as a control group (CG) when compared to Case No. 1. The details are given in Table 3.

Table 3 Key parameters of different cases

No.	Case reference	Coefficient of friction (μ)	W-shaped slope inclination (φ)	Prestressing arrangement	Initial Prestressing	Top mass ratio
1	RSJ-0.05-3-P-0-H	0.05	3°	Partially debonded	0.0 *G*	15
2	CG-0.60-3-P-0-H	0.60	3°	Partially debonded	0.0 *G*	15
3	CG-0.05-0-P-0-H	0.05	0°	Partially debonded	0.0 *G*	15
4	CG-0.05-9-P-0-H	0.05	9°	Partially debonded	0.0 *G*	15
5	CG-0.05-3-F-0-H	0.05	3°	Fully unbonded	0.0 *G*	15
6	CG-0.05-3-P-3-H	0.05	3°	Partially debonded	3.0 *G*	15
7	CG-0.05-3-P-0-L	0.05	3°	Partially debonded	0.0 *G*	3

4.3. Simulation results

Four key performance indicators are evaluated with particular attention to the position of their occurrence: (a) maximum top drift, (b) maximum inter-segmental sliding displacement, (c) maximum vertical gap opening, and (d) residual sliding displacement. The results of seismic time history analysis for the 7 cases are presented in Fig. 9 to Fig. 15. For convenience, labels of the vertical axis are presented as the titles of the subplots and the horizontal axis labels are presented below. The ground is labelled "gr", while the precast segments are labelled from the bottom to the top as "b1" to "b5", so that the inter-segmental displacements can be labelled as gr-b1, b1-b2, etc. The amount of rocking at an interface is shown in terms of the inter-segmental gap opening at the surface.

Among the 7 cases studied, most are provided with partially debonded tendons carrying negligible force, i.e. 0.0 *G* and carrying the regular top mass. The seismic excitation shown in Fig. 8(c) indicates that strong shaking is mainly concentrated in the period from 5 seconds to 25 seconds after commencement of seismic excitation. In Case No. 1 with relatively smooth W-shaped interfaces of mild inclination as shown in Fig. 9, although the inter-segmental displacements and top drift can be quite high within the first 20 seconds, they tend to stabilise afterwards with only a few mm of residual inter-segmental sliding displacement observed at an interface. In Case No. 2 with relatively rough W-shaped interfaces of mild inclination as shown in Fig. 10, the inter-segmental displacements and top drift are seen to be quite high and continue to oscillate for a long time. In Case No. 3 with relatively smooth flat interfaces as shown in Fig. 11, after a short period of strong sliding movements, the inter-segmental sliding displacements and top drift tend to stabilise at fairly large residual values. In Case No. 4 with relatively smooth W-shaped interfaces of moderate inclination as shown in Fig. 12, the inter-segmental displacements and top drift are seen to be quite high and continue to oscillate for a long time. In Case No. 5 with relatively smooth W-shaped interfaces of mild inclination and fully unbonded tendon throughout the column height as shown in Fig. 13, the performance is similar to that in Case 1 with partially debonded tendons, but the inter-segmental displacements and top drift in Case No. 5 tend to be larger. In Case No. 6 with relatively smooth W-shaped interfaces of mild inclination and a relatively high prestressing force of 3.0 *G* as shown in Fig. 14, the inter-segmental displacements and top drift continue to oscillate for a long time. In Case No. 7 with relatively smooth W-shaped interfaces of mild inclination and a lower top mass as shown in Fig. 15, the performance is similar to that in Case No. 1 with the regular top mass, but the inter-segmental displacements and top drift in Case No. 7 tend to be even smaller.

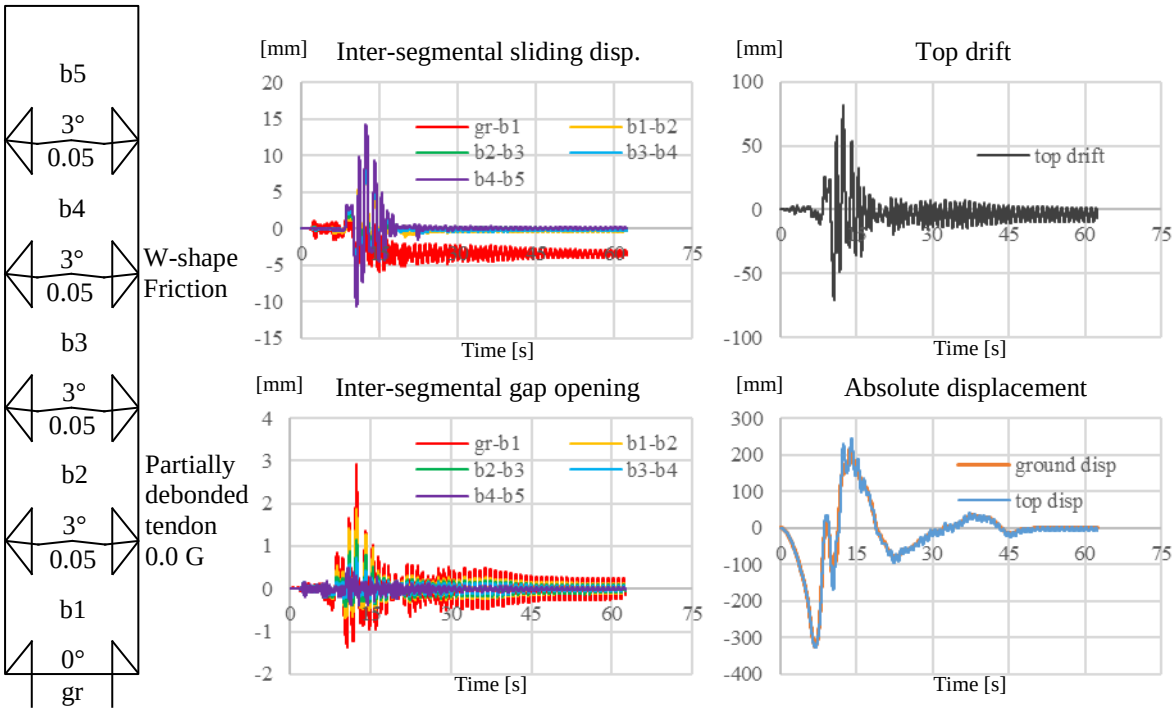

Fig. 9. Case No. 1: Schematic layout and responses of column RSJ-0.05-3-P-0-H under LCN_345 earthquake (PGA normalized to 1.0*g*)

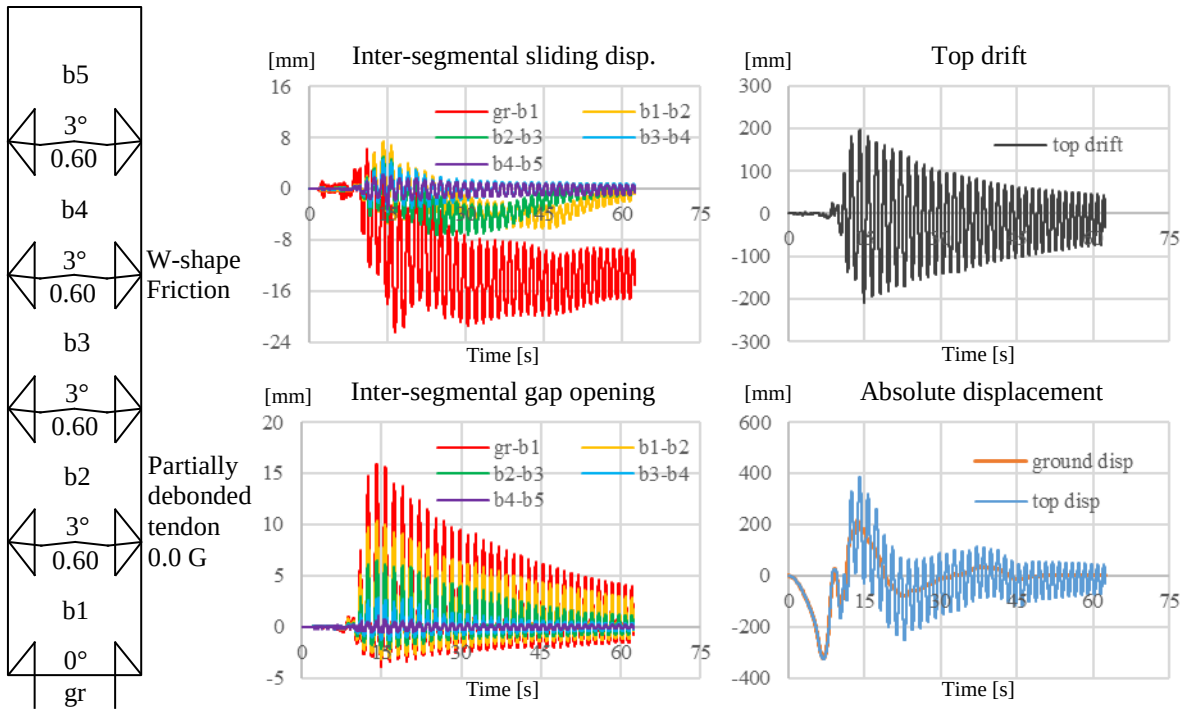

Fig. 10. Case No. 2: Schematic layout and responses of column CG-0.60-3-P-0-H under LCN_345 earthquake (PGA normalized to 1.0*g*)

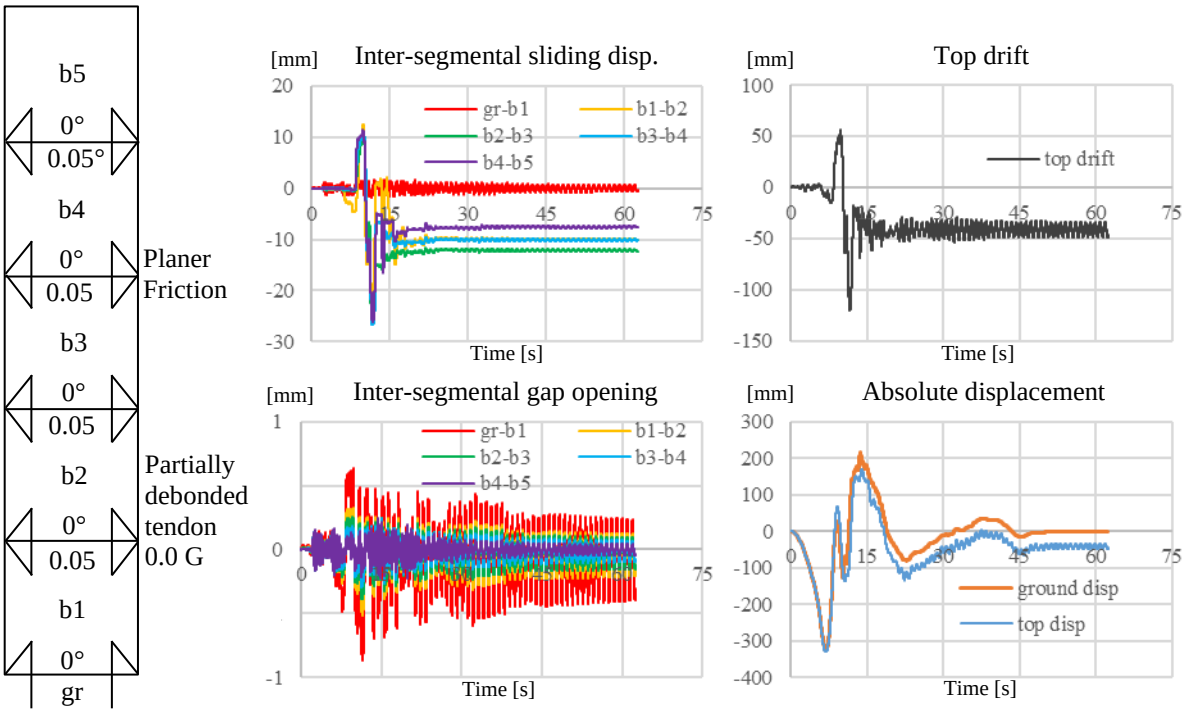

Fig. 11. Case No. 3: Schematic layout and responses of column CG-0.05-0-P-0-H under LCN_345 earthquake (PGA normalized to 1.0*g*)

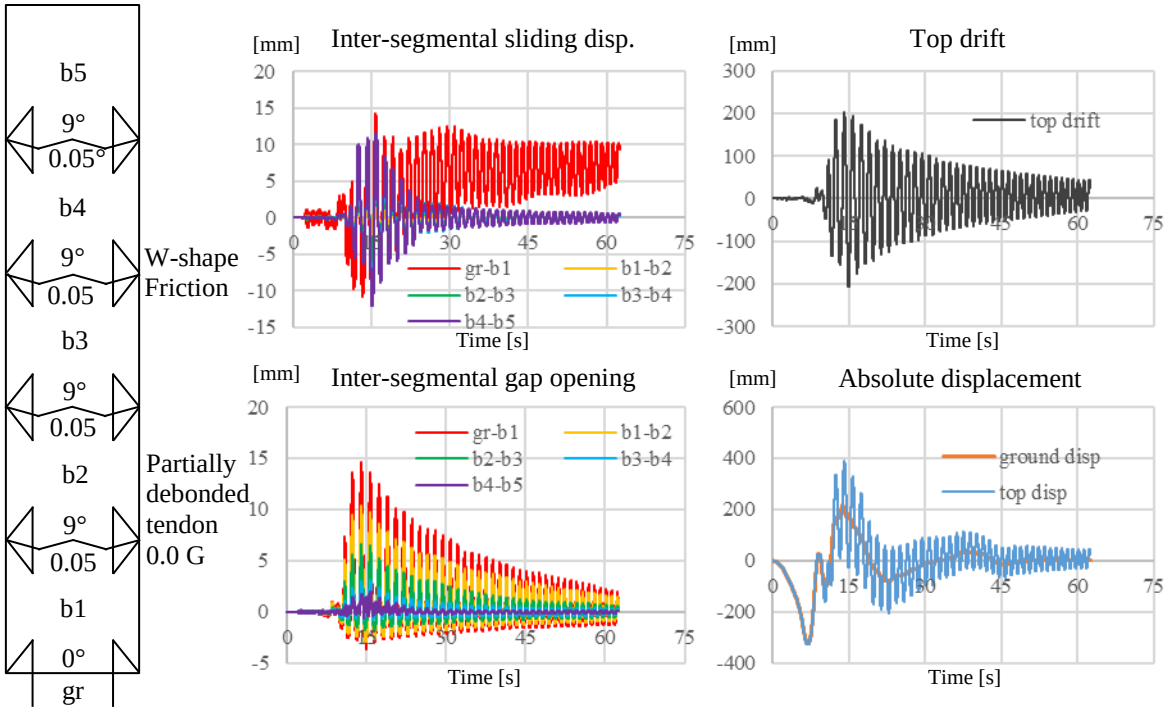

Fig. 12. **Case No. 4: Schematic layout and responses of column CG-0.05-9-P-0-H under LCN_345 earthquake (PGA normalized to 1.0*g*)**

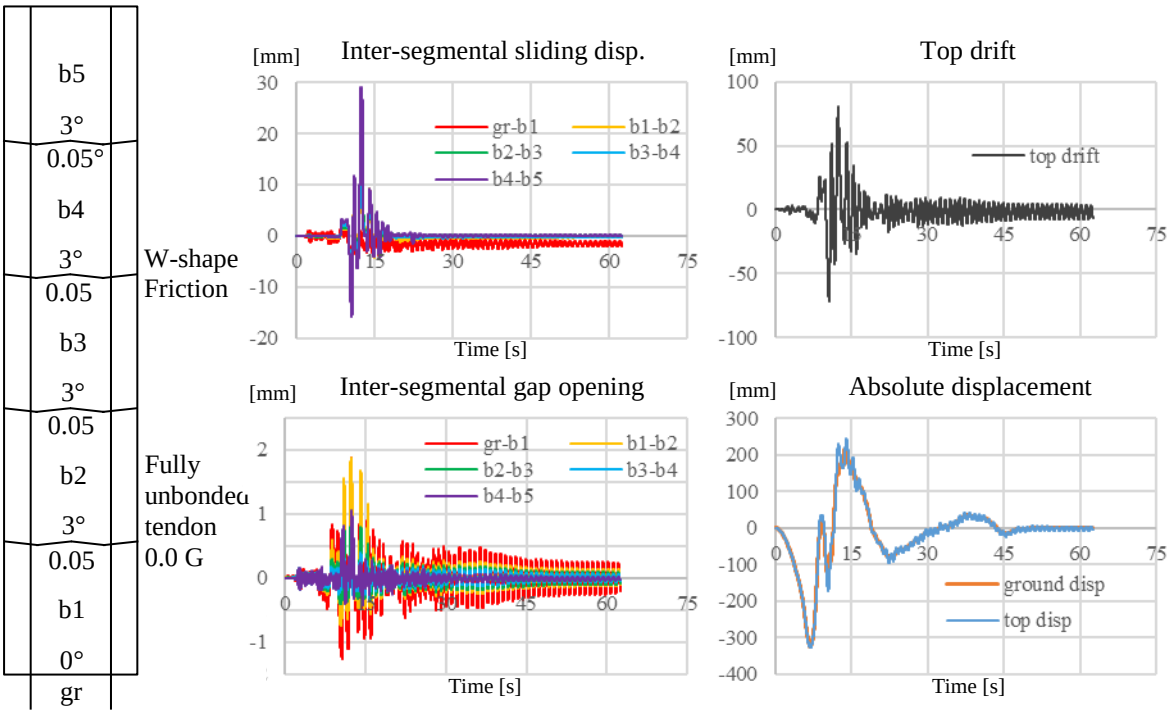

Fig. 13. **Case No. 5: Schematic layout and responses of column CG-0.05-3-F-0-H under LCN_345 earthquake (PGA normalized to 1.0*g*)**

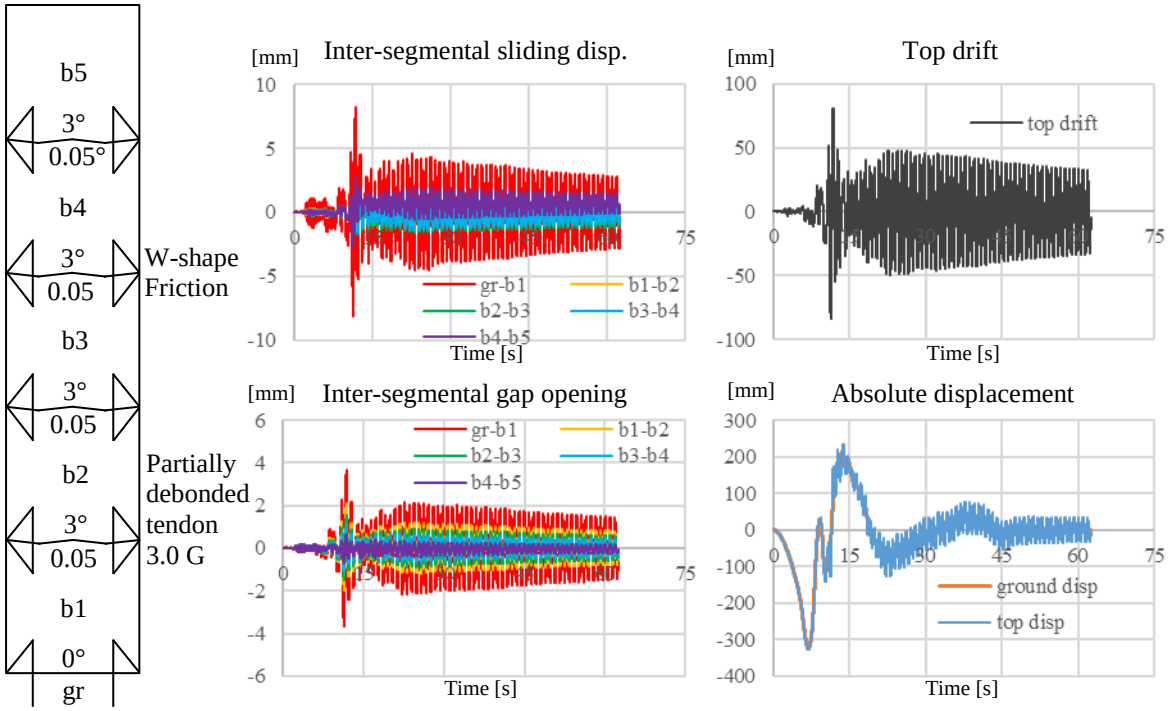

Fig. 14. **Case No. 6: Schematic layout and responses of column CG-0.05-3-P-3-H under LCN_345 earthquake (PGA normalized to 1.0*g*)**

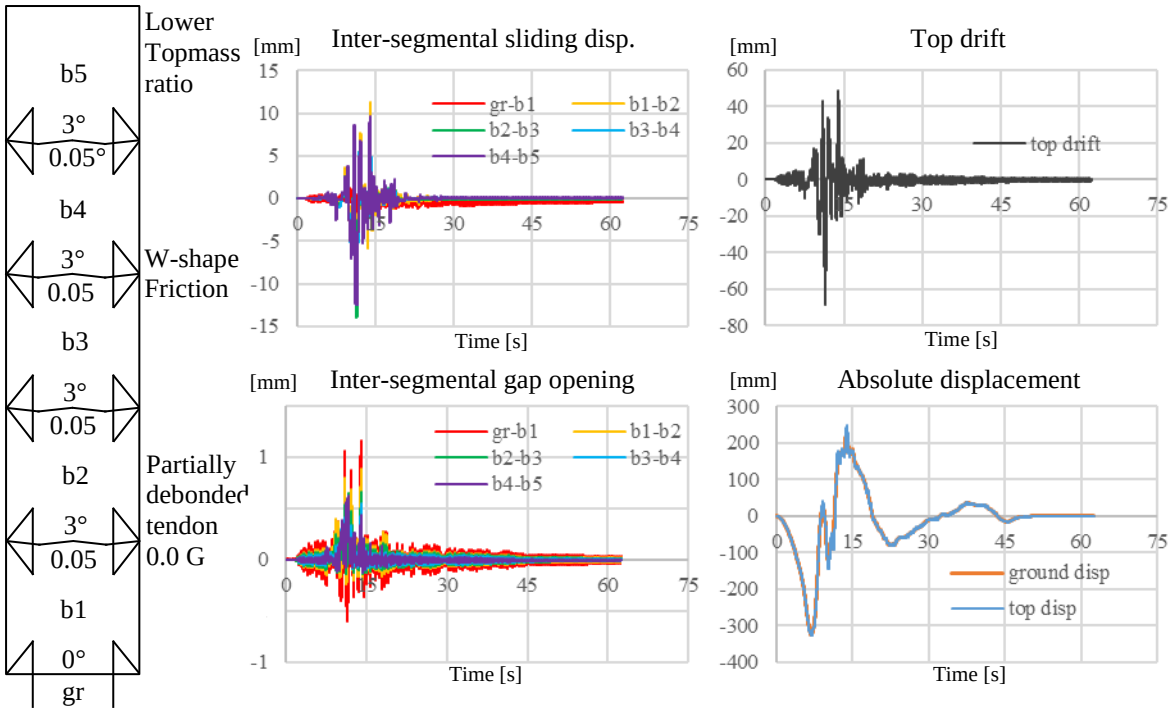

Fig. 15. **Case No. 7: Schematic layout and responses of column CG-0.05-3-P-0-L under LCN_345 earthquake (PGA normalized to 1.0*g*)**

Generally, the occurrence of sliding behaviour at the above-ground joints would effectively mitigate the rocking response of the columns under LCN_345 earthquake input, normally leading to a much smaller top drift and less obvious vibration after the cessation of earthquake, thus achieving satisfactory seismic isolation and better energy dissipation in the whole structure. Indeed, in all the 7 cases studied, the residual variation of drift after the cessation of the earthquake input (i.e. last 15 seconds) continues due to the low energy dissipation from pure rocking behaviour. It is observed from Fig. 9, Fig. 11, Fig. 13 and Fig. 15 that, in Case Nos. 1, 3, 5 and 7, respectively, the drift attenuation is significant upon initiation of inter-segmental sliding, and the residual drift vibration in these 4 cases are minor as compared with those in the other 3 cases. The higher tendency observed for some of the columns to rock may be attributed to the higher equivalent inter-segmental resistance resulting from either a higher CoF at joint interface in Case No. 2 (Fig. 10), a higher inclination of the W-shaped joint interface in Case No. 4 (Fig. 12), or a higher tendon force in Case No. 6 (Fig. 14).

Particularly for Case No. 3, despite the smaller inter-segment gap opening as compared to that in Case No. 1, the sliding behaviour in a column with horizontal planar joint interfaces would ultimately leave noticeable residual sliding displacements. Similarly, a smaller inter-segment gap opening is also observed in Case No. 5. However, compared to the partially debonded tendons in Case No. 1, the fully unbonded tendons in Case No. 5 have weakened the interaction between adjacent segments, leading to a much larger inter-segment sliding displacement especially at the higher joints, but this is barely possible considering the duct size.

An excessive drift with a higher percentage of maximum transient rocking behaviour would probably result in severe local damage at the concrete compression zone. However, moderate rocking behaviour is actually favourable due to its intrinsic self-centring performance. As summarized in Fig. 16, the seismic performance of columns in Case Nos. 1 and 7 with resettable sliding joints outperform the others in various attributes, including (a) a tolerable maximum top drift, (b) a smaller percentage of transient rocking and possibly less prone to local compression damage, and (c) a much smaller residual sliding displacement. The percentage of this resettable sliding behaviour can be further increased with a smaller top mass ratio as demonstrated in Case No. 7.

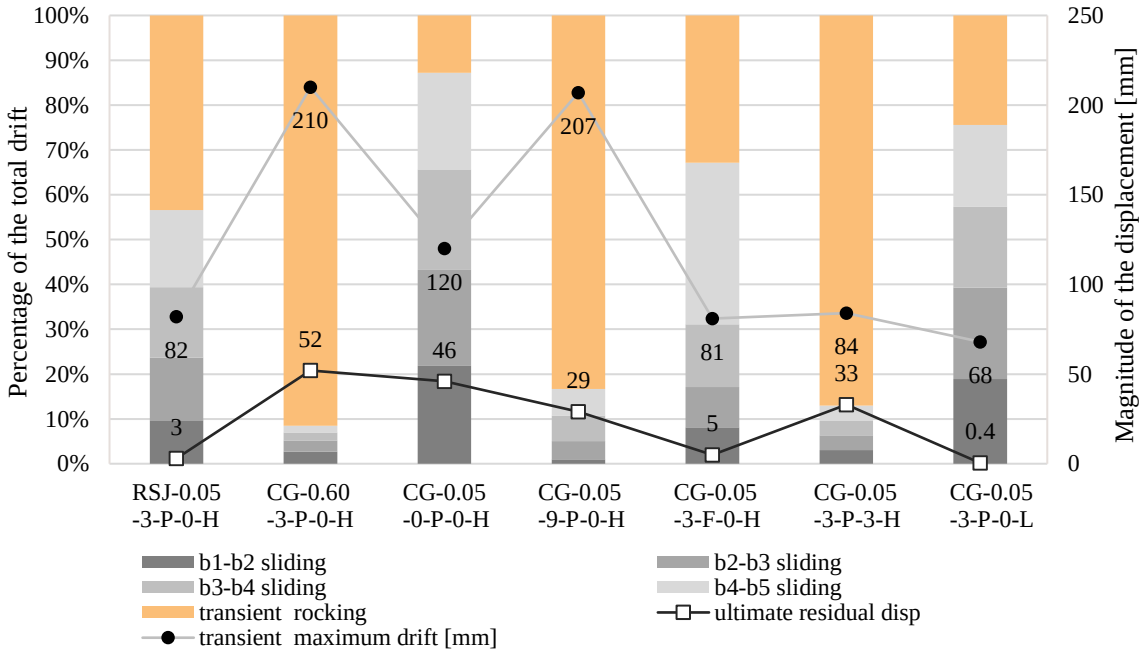

Fig. 16. Transient motion components and drift values of columns at maximum drift condition

5. Conclusions

The superior seismic performance of ancient Chinese timber pagodas with mortise-tenon joints and bracket sets has been examined. The inspiration has been utilised to develop a new design of precast segmental bridge columns with

resettable sliding joints. Simplified 2D numerical models have been established for time-history analyses to capture their dynamic behaviour. Based on the results, the following conclusions can be drawn.

The enlarged gap between the mortise and tenon caused by severe seismic loading would render the mortise-tenon joints more flexible compared to the initial state, subsequently achieving a higher lateral flexibility of the whole structure under an earthquake. This adaptive lateral flexibility is largely reproduced by the low-friction interface at the resettable sliding joints of precast segmental columns.

A smart store-and-release energy transformation mechanism is found in ancient pagodas subject to horizontal displacement in the accompanying uneven uplift movement of a typical floor resulting in its centroid moving along a pendulum orbit. This guided resetting behaviour is largely reproduced by the W-shaped gentle guide keys at the low-friction resettable sliding joints.

The hybrid sliding and rocking behaviour of precast segmental columns with resettable sliding joints is captured by a simplified numerical model incorporating Flat Slider Bearing Elements and co-rotational Truss Elements in the OpenSees environment. The unfavourable rocking behaviour (with low energy dissipation) can be largely alleviated by introducing a sliding-type seismic isolation mechanism to the precast segmental column.

The use of low initial tendon forces and low-friction interfaces in precast segmental columns with resettable sliding joints of mild inclination can facilitate better seismic isolation and resetting performance. Adopting the partially debonded tendon arrangement will further help in optimizing the sliding displacement among all the joints.

Acknowledgments

The work described here has been partially supported by the Ministry of Science and Technology, China (Project No.: 2019YFB1600702). The OpenSees script has been developed based on the example coded by Andreas Schellenberg available at https://opensees.berkeley.edu/wiki/index.php/Flat_Slider_Bearing_Element.

References

[1] Kurama YC, Sritharan S, Fleischman RB, et al. (2018), Seismic-resistant precast concrete structures: State of the art. American Society of Civil Engineers. 10.1061/(ASCE)ST.1943-541X.0001972

[2] Chou CC, Chang HJ and Hewes JT (2013), Two-plastic-hinge and two dimensional finite element models for post-tensioned precast concrete segmental bridge columns, Engineering Structures, 46: 205-217. https://doi.org/10.1016/j.engstruct.2012.07.009

[3] Li C, Hao H and Bi K (2018a), Seismic performance of precast concrete-filled circular tube segmental column under biaxial lateral cyclic loadings, Bulletin of Earthquake Engineering, August 2018. https://doi.org/10.1007/s10518-018-0443-4

[4] Ou YC, Chiewanichakorn M, Aref AJ and Lee GC (2007), Seismic performance of segmental precast unbonded posttensioned concrete bridge columns, Journal of Structural Engineering, 133(11): 1636-1647. https://doi.org/10.1061/(asce)0733-9445(2007)133:11(1636)

[5] Sideris P (2012), Seismic Analysis and Design of Precast Concrete Segmental Bridges, PhD Dissertation, Department of Civil, Structural and Environmental Engineering, State University of New York at Buffalo, Buffalo, NY.

[6] Sideris P, Aref AJ and Filiatrault A (2014), Quasi-static cyclic testing of a large-scale hybrid sliding-rocking segmental column with slip-dominant joints, Journal of Bridge Engineering, 19(10): 04014036. https://doi.org/10.1061/(asce)be.1943-5592.0000605

[7] Sideris P, Aref AJ and Filiatrault A (2014), Large-scale seismic testing of a hybrid sliding-rocking posttensioned segmental bridge system, Journal of Structural Engineering, 140(6): 04014025. https://doi.org/10.1061/(asce)st.1943-541x.0000961

[8] Ou YC, Wang PH, Tsai MS, Chang KC, Lee GC (2009), Large-scale experimental study of precast segmental unbonded posttensioned concrete bridge columns for seismic regions. Journal of Structural Engineering, 136(3): 255–64. https://doi.org/10.1061/(asce)st.1943-541x.0000110

[9] Thonstad T, Mantawy IM, Stanton JF, Eberhard MO, Sanders DH (2016), Shaking table performance of a new bridge system with pretensioned rocking columns. J Bridge Eng, 21(4): 04015079. https://doi.org/10.1061/(asce)be.1943-5592.0000867

[10] Bu ZY, Ou YC, Song JW, Zhang NS, Lee GC (2015), Cyclic loading test of unbonded and bonded posttensioned precast segmental bridge columns with circular section. J Bridge Eng, 21(2), 04015043. https://doi.org/10.1061/(asce)be.1943-5592.0000807

[11] Song LL, Guo T, & Cao ZL (2015), Seismic response of self-centering prestressed concrete moment resisting frames with web friction devices. Soil Dynamics and Earthquake Engineering, 71, 151-162. https://doi.org/10.1016/j.soildyn.2015.01.018

[12] Song LL, Guo T, & Chen C (2014), Experimental and numerical study of a self-centering prestressed concrete moment resisting frame connection with bolted web friction devices. Earthquake engineering & structural dynamics, 43(4), 529-545. https://doi.org/10.1002/eqe.2358

[13] Lin K, Lu X, Li Y, & Guan H (2019), Experimental study of a novel multi-hazard resistant prefabricated concrete frame structure. Soil Dynamics and Earthquake Engineering, 119, 390-407. https://doi.org/10.1016/j.soildyn.2018.04.011

[14] Qu H, Li T, Wang Z, Wei H, Shen J, & Wang H (2018), Investigation and verification on seismic behavior of precast concrete frame piers used in real bridge structures: Experimental and numerical study. Engineering Structures, 154, 1-9. https://doi.org/10.1016/j.engstruct.2017.10.069

[15] Jin K, Song S, Kitayama K, & Hao L (2019), Detailed evaluation of the ultimate flexural states of beams in unbonded precast prestressed concrete frames. Bulletin of Earthquake Engineering, 17(3), 1495-1519. https://doi.org/10.1007/s10518-018-0504-8

[16] Chen Z, Zhu E, Pan J, & Wu G (2016), Energy-dissipation performance of typical beam-column joints in Yingxian Wood Pagoda: experimental study. Journal of Performance of Constructed Facilities, 30(3), 04015028. https://doi.org/10.1061/(asce)cf.1943-5509.0000771

[17] Wu Y, Song X, Gu X, & Luo L (2018), Dynamic performance of a multi-story traditional timber pagoda. Engineering Structures, 159, 277-285. https://doi.org/10.1016/j.engstruct.2018.01.003

[18] Xie Q, Wang L, Zhang L, Hu W, & Zhou T (2019), Seismic behaviour of a traditional timber structure: shaking table tests, energy dissipation mechanism and damage assessment model. Bulletin of earthquake engineering, 17(3), 1689-1714. https://doi.org/10.1007/s10518-018-0496-4

[19] Wu Y, Song X, & Li K (2018), Compressive and racking performance of eccentrically aligned dou-gong connections. Engineering Structures, 175, 743-752. https://doi.org/10.1016/j.engstruct.2018.08.054

[20] Chen Z, Zhu E, Lam F, & Pan J (2014), Structural performance of Dou-Gong brackets of Yingxian Wood Pagoda under vertical load–An experimental study. Engineering structures, 80, 274-288. https://doi.org/10.1016/j.engstruct.2014.09.013

[21] Ma L, Xue J, Dai W, Zhang X, & Zhao X (2020), Moment-rotation relationship of mortise-through-tenon connections in historic timber structures. Construction and Building Materials, 232, 117285. https://doi.org/10.1016/j.conbuildmat.2019.117285

[22] Li X, Zhao J, Ma G, & Chen W (2015), Experimental study on the seismic performance of a double-span traditional timber frame. Engineering Structures, 98, 141-150. https://doi.org/10.1016/j.engstruct.2015.04.031

[23] Sha B, Wang H, & Li A (2019), The Influence of the Damage of Mortise-Tenon Joint on the Cyclic Performance of the Traditional Chinese Timber Frame. Applied Sciences, 9(16), 3429. https://doi.org/10.3390/app9163429

[24] Meng X, Li T, & Yang Q (2019), Experimental study on the seismic mechanism of a full-scale traditional Chinese timber structure. Engineering Structures, 180, 484-493. https://doi.org/10.1016/j.engstruct.2018.11.055

[25] Mikey (2021) Retrieved from https://unsplash.com/@daxtersky (in accordance with terms and condition of license).

[26] Chui YH, & Li Y (2005), Modeling timber moment connection under reversed cyclic loading. Journal of Structural Engineering, 131(11), 1757-1763. https://doi.org/10.1061/(asce)0733-9445(2005)131:11(1757)

[27] Zhang XC, Xue JY, Zhao HT, & Sui Y (2011), Experimental study on Chinese ancient timber-frame building by shaking table test. Structural Engineering and Mechanics, 40(4), 453-469. https://doi.org/10.12989/sem.2011.40.4.453

[28] Xue JY, Wu ZJ, Zhang FL, & Zhao HT (2015), Seismic damage evaluation model of Chinese ancient timber buildings. Advances in Structural Engineering, 18(10), 1671-1683. https://doi.org/10.1260/1369-4332.18.10.1671

[29] Huang H, Sun Z, Guo T, & Li P (2017), Experimental study on the seismic performance of traditional Chuan-Dou style wood frames in Southern China. Structural Engineering International, 27(2), 246-254. https://doi.org/10.2749/101686617x14881932435817

[30] D'Ayala DF, & Tsai PH (2008), Seismic vulnerability of historic Dieh–Dou timber structures in Taiwan. Engineering structures, 30(8), 2101-2113. https://doi.org/10.1016/j.engstruct.2007.11.007

[31] Li Z, Que Y, Zhang X, Teng Q, Hou T, Liu Y, ... & Komatsu K (2018), Shaking Table Tests of Dou-gong Brackets on Chinese Traditional Wooden Structure: A Case Study of Tianwang Hall, Luzhi, and Ming Dynasty. BioResources, 13(4), 9079-9091. https://doi.org/10.15376/biores.13.4.9079-9091

[32] Yi J, & Li JZ (2019), Effect of seismic-induced bearing uplift of a cable-stayed bridge. Journal of Bridge Engineering, 24(3), 04018125. https://doi.org/10.1061/(asce)be.1943-5592.0001342

[33] Zhou Q, & Yan WM (2008), Study on Parameters of Quake-Proof for Shen-Wu Gate in the Forbidden City in China. The 14th World Conference on Earthquake Engineering, October 12-17, Beijing, China.

[34] Liu YQ, Yuan Y, Liang F & Au FTK (2020), Resetting Response of Precast Segments with Gently Keyed Interface under Seismic Action. Earthquake Engineering & Structural Dynamics, September 2020. https://doi.org/10.1002/eqe.3348

[35] Au FTK, Liu YQ, Yuan Y, Su RKL, Lam NTK (2019), Seismic Performance of Precast Segmental Bridge Columns with Resettable Sliding Joints: Feasibility Study. Proceedings of the Bridge Engineering Institute Conference – Frontiers of Bridge Engineering – Honolulu, Hawaii, July 2019.

[36] Hossain MA, Totoev Y and Masia MJ (2016), Friction on mortar-less joints in semi interlocking masonry. Conference on Brick and Block Masonry – Trends, Innovations and Challenges – Modena, da Porto & Valluzzi (Eds), August 2016. https://doi.org/10.1201/b21889-203

[37] Liu YQ, Yuan Y, Au FTK, Su RKL, Lam NTK (2019), Seismic Performance of Precast Segmental Bridge Columns with Resettable Sliding Joints: Friction at Interface. Proceedings of the Bridge Engineering Institute Conference – Frontiers of Bridge Engineering – Honolulu, Hawaii, July 2019.

[38] McKenna F, Fenves GL, Scott MH & Jeremic B (2000), Open system for earthquake engineering simulation (OpenSees), Univ. of California, Berkeley, CA.

[39] Salehi M, Sideris P, & Liel AB (2017), Numerical simulation of hybrid sliding-rocking columns subjected to earthquake excitation. Journal of Structural Engineering, 143(11), 04017149. https://doi.org/10.1061/(asce)st.1943-541x.0001878

[40] Ahmadi E & Kashani MM (2020), Numerical investigation of nonlinear static and dynamic behaviour of self-centring rocking segmental bridge piers. Soil Dynamics and Earthquake Engineering, 128, 105876. https://doi.org/10.1016/j.soildyn.2019.105876

[41] Maffei J, Fathali S, Telleen K, Ward R & Schellenberg A (2014), Seismic design of ballasted solar arrays on low-slope roofs. Journal of Structural Engineering, 140(1), 04013020. https://doi.org/10.1061/(asce)st.1943-541x.0000865

[42] Bao Y (2020), Modeling Dynamic Behavior of Stacked Sliding-Rocking Rigid Blocks Subjected to Base Excitation. International Journal of Structural Stability and Dynamics, 20(05), 2050070. https://doi.org/10.1142/s0219455420500704